Comblike Alkyl Esters of Biosynthetic Poly(γ-glutamic acid). 2. Supramolecular Structure and Thermal Transitions

Margarita Morillo,† Antxon Martínez de Ilarduya,‡ Abdelilah Alla,§ and Sebastián Muñoz-Guerra*

Departament d'Enginyeria Química, ETSEIB, Universitat Politècnica de Catalunya, Diagonal 647, Barcelona 08028, Spain

Received April 23, 2003; Revised Manuscript Received July 14, 2003

ABSTRACT: The solid-state structure of comblike poly(α-*n*-alkyl γ-glutamate)s derived from bacterial poly(γ-glutamic acid) (PAAG-*n*, *n* being the number of carbons contained in the linear alkyl side chain) was investigated for even values of *n* between 12 and 22. Two series, one with a D:L enantiomeric ratio of approximately 9:1 and the other with a nearly racemic composition, were examined. The thermal transitions and the structures involved therein were characterized by DSC, polarizing infrared, X-ray and electron diffraction, and ^{13}C CP/MAS NMR. In all cases and within the whole examined range of temperature, the polypeptide main chain was arranged in an α-helix-like conformation. A first-order transition occurring at a temperature T_1 between 20 and 80 °C and interconverting two well-defined phases, A and B, was characterized for PAAG-*n* with $n \geq 14$. Phase A is a biphasic structure consisting of layers of polypeptide helices separated by a paraffinic pool of alkyl side chains. The layer periodicity was found to increase steadily from 2.7 to 3.7 nm according to a structure in which the alkyl side groups are partially crystallized, oriented nearly normal to the layers, and extensively interdigitized. Phase B retains the layered structure present in phase A but with side chains being in a disordered state. A second first-order transition, leading to a third phase C at a temperature T_2 near 100 °C, was characterized for PAAG-*n* with $n \geq 18$. Phase C is thought to be a nematic structure consisting of a quasi-hexagonal packing of helical polypeptide rods lacking axial register. Although no clear differences in the structure of any of the three phases were detected between the two investigated series, the response to the thermal treatment was significantly affected by the stereochemistry of the PAAG-*n*. Crystallization from the melt was favored in the DL series, the dimensional changes involved in the A−B transition showed opposite sign for D and DL polymers, and the B−C transition was much more noticeable in the DL series.

Introduction

Comblike polypeptides bearing long linear alkyl side groups are currently of great interest for their ability to adopt supramolecular structures suitable for the development of new materials with advanced properties.[1] These systems consist of a rodlike main chain helix and a flexible side chain that can be either disordered or crystallized depending on both chain length and temperature. Above the melting point of the alkyl side chain, comblike polypeptides behave as if they were lyotropic liquid crystals with the molten paraffinic phase playing the role of a solvent. Some of these polypeptides are distinguished by their ability to display striking thermochromic effects reminiscent of cholesteric structures.[2,3]

A fair amount of research has been carried out on comblike poly(γ-alkyl α,L-glutamate)s and poly(β-alkyl α,L-aspartate)s.[1] Watanabe et al.[4] reported for the first time that the supramolecular structure adopted by poly(γ-alkyl α,L-glutamate)s is largely determined by the size of the side chain. Whereas the smaller members crystallize in a three-dimensional crystal lattice, those members containing 10 or more carbon atoms in the alkyl side group tend to be arranged in a two-dimensional biphasic layered structure. This is described as made up of sheets of α-helices packed side-by-side, with the polymethylene side chains crystallized in a separate paraffinic phase. The synthesis, structure, and properties of these systems have been appropriately reviewed.[5] Identical arrangements have recently been shown to exist also in comblike poly(α-alkyl β,L aspartate)s.[6] These are poly(β-peptide)s that may adopt rigid α-helix-type conformations, a remarkable feature that was first evidenced some years ago[7] and which has been corroborated in the past few years by definite spectroscopic and crystallographic results afforded in the structural analysis of oligo(β-peptide)s.[8]

In this paper, we are concerned with poly(γ-peptide)s, a second class of unconventional polypeptides, which can be envisaged as nylon-4 derivatives. Poly(γ-peptide)s have two additional methylenes in the main chain of the repeating unit when compared with poly(α-peptide)s. Despite the much higher flexibility inherent in the poly(γ-peptide) backbone, an intramolecular hydrogen-bonded 5/2 helix has been found to occur in the synthetic methyl and benzyl esters of poly(γ,L-glutamic acid)[9] and in oligo(γ,L-amino acid)s.[10] A very recent study[11] carried out on poly(α-benzyl γ-glutamate)s prepared from biosynthetic poly(γ-glutamic acid) with varying D:L ratio has revealed that the occurrence of a helical structure is compatible with an enantiomerically heterogeneous composition, a fact consistent with the block stereochemical microstructure shown to be present in poly(γ-glutamate)s of microbial origin.[12] A helical conformation containing 37 residues per 10 turns has also been observed in these cases. Furthermore, a 17/5 helix, very similar in topology to the 37/10 helix, has

* Corresponding author: E-mail: sebastian.munoz@upc.es.
† E-mail: Margarita.Morillo@upc.es.
‡ E-mail: antxon.martinez.de.ilarduia@upc.es.
§ E-mail: Abdel.Alla@upc.es.

10.1021/ma0345201 CCC: $25.00 © 2003 American Chemical Society
Published on Web 09/12/2003

been proposed for poly(γ-glutamic acid) in the nonionized form.[13]

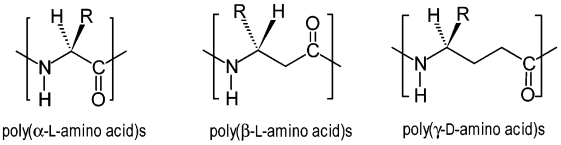

We have recently reported on the synthesis and characterization of comblike poly(α-*n*-alkyl γ-glutamate)s,[14] abbreviated as PAAG-*n*, where *n* stands for the number of carbon atoms contained in the linear alkyl side chain. These poly(γ-glutamate)s were prepared from bacterially produced poly(γ-glutamic acid) in a two-stage esterification procedure. Two series of PAAG-*n*—one with a nearly racemic composition, denoted as PAA(DL)G-*n*, and the other with a nearly optically pure D composition, denoted as PAA(D)G-*n*—were examined for even values of *n* ranging from 12 to 22. It was there shown by NMR that these PAAG-*n* are able to adopt helical conformations in solution, and preliminary X-ray results revealed that in the solid state they took up the layered arrangement typical of comblike polymers. In this work, we wish to report on the structure of these comblike poly(γ-peptide)s in full detail, with the study being focused on the characterization of the different phases that are generated by thermal effects. A set of complementary analytical techniques, including DSC, ^{13}C CP/MAS NMR, polarizing infrared spectroscopy, and electron and X-ray diffraction, has been applied to attain a comprehensive description of the structure present in each phase. Results are properly referenced to those previously reported for other comblike polypeptides, poly(γ-alkyl α,L-glutamate)s[4] and poly(α-alkyl β,L-aspartate)s,[6] with the purpose of correlating structure and chemical constitution.

Experimental Section

Materials and Synthesis. All chemicals were obtained commercially from either Aldrich or Merck. They were analytical grade or higher, and used without further purification. Solvents to be used under anhydrous conditions were dried by standard methods. The synthesis and chemical characterization of the PAAG-*n* used in this work were described in full detail in a previous paper.[14] In brief, bacterially produced poly(γ-glutamic acid) was esterified to poly(α-ethyl γ-glutamate), and this compound was then converted into PAAG-*n* by transesterification with the corresponding alkanols. Two poly(γ-glutamic acid)s differing in the enantiomeric composition were used to prepare the two respective series of PAAG-*n*. PGG(DL)A with a D:L ratio of 60:40 and an average molecular weight of 390 000 was kindly supplied by Dr. Kubota of Meiji Co.. PGG(D)A with a D:L ratio of 88:12 was prepared in our laboratory by fermentation of medium E with *B. licheniformis*, and its original molecular weight was reduced to 340 000 by microwave irradiation, as reported in detail elsewhere.[15] The synthesis scheme leading to the PAAG-*n* investigated in this work is outlined in Figure 1, and their most-relevant data are given in Table 1.

Measurements. All polymer films used in this study were prepared by casting from chloroform and dried under vacuum. To induce orientation, as needed for polarizing infrared and X-ray diffraction, rectangular pieces of these films were subjected to uniaxial mechanical stretching under controlled temperature. Dichroic spectra were recorded in a Perkin-Elmer FTIR-2000 instrument equipped with an external gold polarizer. Dichroic ratios were determined from the absorbance measured for the parallel and perpendicular orientations of the film to the infrared polarization vector. ^{13}C CP/MAS NMR spectra were recorded from powder samples in the temperature range 20−80 °C on a Bruker AMX-300 NMR instrument provided with a variable temperature unit. Calorimetric measurements were performed with a Perkin-Elmer Pyris I DSC instrument operating under a nitrogen atmosphere and calibrated with indium. Sample weights of about 2−5 mg were heated or cooled at rates of ±10 °C min^{-1}. X-ray diffraction patterns were taken from both oriented and unoriented polymer films in a Statton-type camera using nickel-filtered Cu Kα radiation of wavelength 0.1542 nm. The patterns were recorded on flat photographic films and were calibrated with molybdenum sulfide (d_{002} = 0.6147 nm). X-ray thermodiffractograms were recorded from unoriented polymer films in a Siemens D-500 diffractometer using Cu Kα radiation and provided with a TPK-A Park heating stage and a scintillation counter. Electron diffraction patterns were recorded from ultrathin films prepared by casting from chloroform on a water surface. A Philips EM-301 instrument operating in the selected area mode and calibrated with gold was used for this purpose.

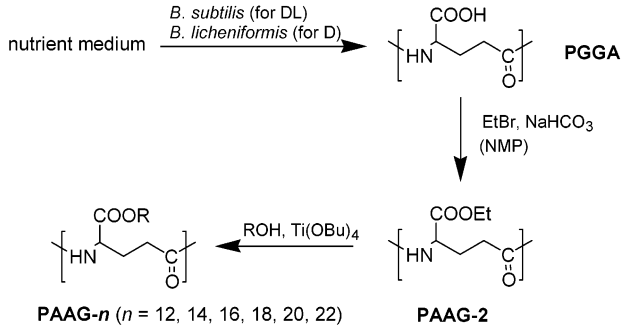

Figure 1. Scheme for the synthesis of PAAG-*n*.

Table 1. Data for Poly(α-*n*-alkyl γ-glutamate)s Studied in This Work

PAAG-*n*	R	M_o (UCR)	$M_w \times 10^{-3}$ [a]	PD	D:L[b]	ρ (g mL^{-1})[c]
PAA(D)G-12	*n*-$C_{12}H_{25}$	297	150	1.31	88:12	1.01
PAA(DL)G-12			150	1.27	60:40	
PAA(D)G-14	*n*-$C_{14}H_{29}$	325	250	1.33	88:12	1.00
PAA(DL)G-14			89	1.22	60:40	
PAA(D)G-16	*n*-$C_{16}H_{33}$	353	140	1.36	88:12	1.02
PAA(DL)G-16			100	1.40	60:40	
PAA(D)G-18	*n*-$C_{18}H_{37}$	381	170	1.42	88:12	1.02
PAA(DL)G-18			32	1.52	60:40	
PAA(D)G-20	*n*-$C_{20}H_{41}$	409	100	1.40	88:12	1.01
PAA(DL)G-20			86	1.45	60:40	
PAA(D)G-22	*n*-$C_{22}H_{45}$	437	66	1.30	88:12	1.01
PAA(DL)G-22			42	1.28	60:40	

[a] Molecular weight determined by SEC/LS. [b] Enantiomeric composition determined by HPLC. [c] Density measured by flotation in aqueous KBr solution at room temperature.

Results and Discussion

PAAG-*n* display a good stability to heating, with the onset of thermal decomposition under inert atmosphere appearing in the 310−330 °C range.[14] The reversible heat exchange observed in the 0−100 °C range of DSC traces of PAAG-*n* is undoubtedly due to an endothermic process associated with the melting of the polymethylene side chain. As expected, the position and intensity of the peak steadily increase with the length of the alkyl group. Whereas essentially flat traces were recorded for PAAG-12 and PAA(DL)G-14, sharp peaks with almost linearly increasing enthalpy were obtained for all other members. The second heating DSC traces of PAA(DL)G-*n* showing the melting peak of samples crystallized from the melt are compared in Figure 2.

It should be stressed that almost identical results were obtained in the calorimetric analysis of both PAA-

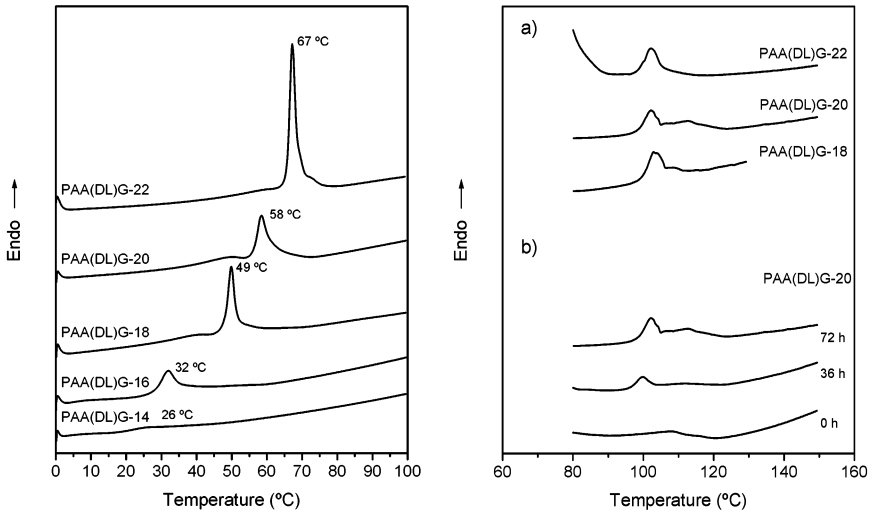

Figure 2. DSC traces of PAAG-*n*. Left: Low-temperature melting peak observed for melt-crystallized samples. Right: The second transition peak observed in the proximity of 100 °C. (a) Comparative traces of the indicated PAA(DL)G-*n* annealed at 88 °C for 72 h. (b) Effect of the annealing time on the peak of PAA(DL)G-20.

Table 2. Calorimetric Data of Transitions A → B and B → C in PAAG-*n*

	A → B transition						B → C transition	
PAAG-*n*	T_1 (°C)[a]	T_1 (°C)[b]	ΔH_1 (cal mol^{-1})[a]	ΔH_1 (cal mol^{-1})[b]	$\Delta S^a/\Delta S^b$ (cal K^{-1}·mol^{-1})	$n_c{}^a/n_c{}^b$	T_2 (°C)	ΔH_2 (cal·mol^{-1})
PAAG-12								
D	n.o.[c]	n.o.	n.o.	n.o.	n.o.	n.o.	n.o.	n.o.
DL	n.o.	n.o.	n.o.	n.o.	n.o.	n.o.	n.o.	n.o.
PAAG-14								
D	n.o.	n.o.	n.o.	n.o.	n.o.	n.o.	n.o.	n.o.
DL	20	26	1290	310	4.4/1.0	1.1/0.4	n.o.	n.o.
PAAG-16								
D	43	41	2460	450	7.8/1.4	2.1/0.9	n.o.	n.o.
DL	38	32	3650	1580	11.7/5.2	3.0/2.1	n.o.	n.o.
PAAG-18								
D	55	39	6190	1550	18.9/5.0	5.2/3.0	n.o.	n.o.
DL	53	49	6040	3350	18.5/10.4	5.0/4.5	99	420
PAAG-20								
D	61	51	9530[d]	2670	28.5/8.2	7.9/5.1	104	32
DL	59	58	7090	4310	21.4/13.0	5.9/5.7	102	328
PAAG-22								
D	72	64	9740	3520	28.9/10.5	8.1/6.8	103	93
DL	71	67	10 210	6430	29.7/18.9	8.5/8.6	102	382

[a] Values estimated from samples prepared by precipitation from solution. [b] Values estimated from samples crystallized from the melt. [c] n.o.: not observed. [d] A value of around 3500 was obtained for one fresh sample obtained by the same procedure.

(D)G-*n* and PAA(DL)G-*n* series, as far as melting of the alkyl side chain is concerned, although in the D series, the tetradecyl derivative failed to show any sign of heat absorption indicative of fusion. The calorimetric data recorded for the two series are given in Table 2 for samples coming from synthesis and for those obtained by isothermal crystallization from the melt. Comparison of these data indicates that neither the position nor the intensity of the melting peak is significantly affected by the enantiomeric composition, the observed small differences being most likely due to experimental inaccuracies rather than to configurational effects. Conversely, the characteristics of the peak were found to be extremely sensitive to the treatment applied for the preparation of the sample. Maximum values were generally obtained from samples coming directly from synthesis, whereas relatively small values were obtained for samples prepared by isothermal crystallization from the melt. Such strong dependence of the melting parameters on thermal history impeded attaining a reliable correlation of T_m and ΔH_m with the value of *n*. The annealing treatment did not prove to be helpful in this regard, due to the difficulties encountered in finding similar relative temperatures of treatment.

The calculated entropy for the T_1 peak follows the expected trend. It increases with *n*, and values are highly comparable to those reported for poly(α-glutamate)s and poly(β-aspartate)s, their similarities becoming closer as the length of the alkyl side chain increases. The fact that neither crystallization of the dodecyl side chain is observed for PAAG-12 nor crystallization of the tetradecyl side chain for PAA(D)G-14 is in disagreement with the behavior observed for analogous members in the other two families of polypeptides. It was noticed previously in the study of comblike PAALA-*n* that the dodecyl side chain was crystallized in PGAG-12 but not in PAALA-12.[6] Such differences bring into evidence that crystallization of the alkyl side chains of comblike polypeptides becomes less feasible as the length of the main chain repeating unit increases, probably due to the increasing difficulty in chain packing caused by the lower density of side groups in the polypeptide. According to what is known to happen in poly(α-glutamate)s and poly(β-aspartate)s, the endot-

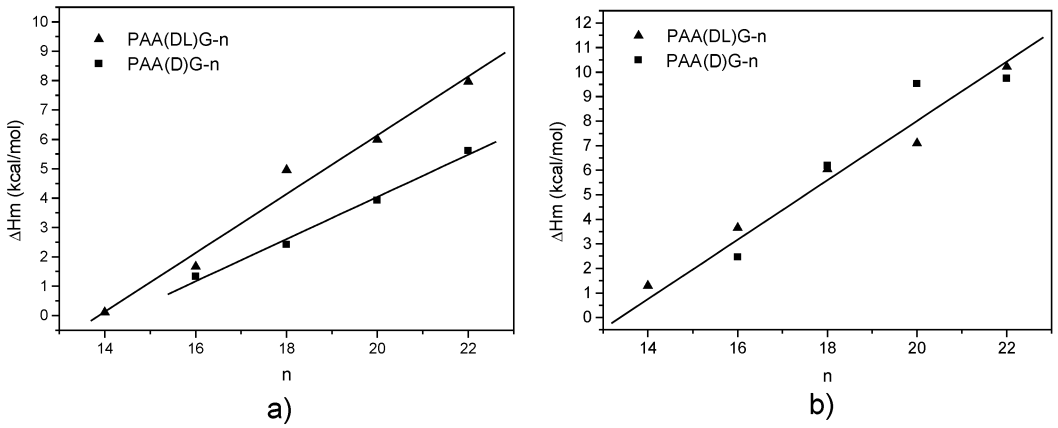

Figure 3. Enthalpy of the A−B transition against number of carbon atoms in the alkyl side chain of PAAG-*n*. (a) Samples prepared by crystallization from the melt. (b) Samples obtained by precipitation from solution.

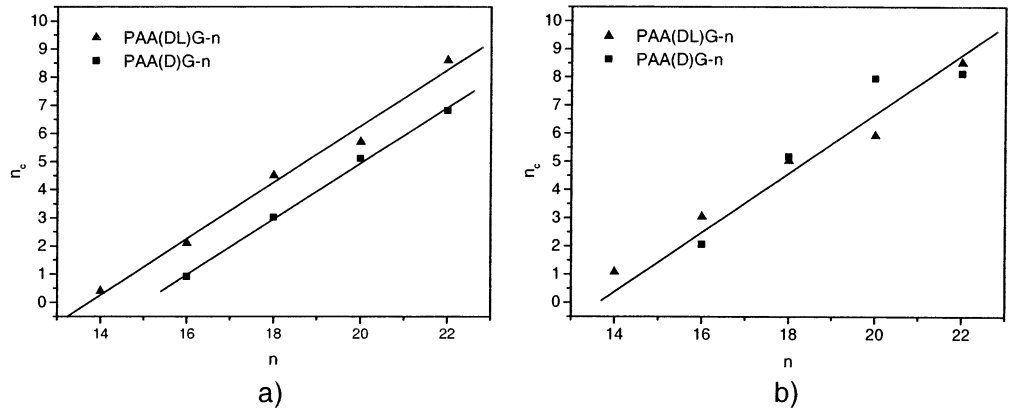

Figure 4. Number of crystallized methylene units as a function of *n*. (a) Samples crystallized from the melt. (b) Samples obtained by precipitation from solution.

hermic peak appearing in the low-temperature region of DSC traces should be interpreted as arising from the melting of the paraffinic nanophase made up of partially crystallized alkyl side chains. This melting temperature, T_1, defines therefore the transition between phases A and B. The structure of these two phases will be discussed below.

The enthalpy of the lower-temperature melting peak of comblike polymers bearing crystallizable side chains is indicative of the number of methylenes participating in the crystalline paraffinic phase (n_c). The variation in enthalpy of the A−B transition with the value of *n* is plotted in Figure 3 for both the D and the DL-series, and for the two types of sample examined in this work. The regression straight line resulting from these data represents the equation established in the literature[16,17] for comblike polymers bearing polymethylene side chains, in which $\Delta H_m(e)$ is the contribution made by the end methyl groups and *k* is the averaged melting enthalpy for each crystallized methylene.

$$\Delta H_m = \Delta H_m(e) + n_c k \qquad (1)$$

The *k* value for PAAG-*n* crystallized from the melt is about 750 and 520 cal CH_2-mol^{-1} for the DL and D series, respectively. These values are far from the 950−1000 cal CH_2-mol^{-1} reported for the melting of linear alkanes and polyethylene crystallized in the rhombic form.[17] They are comparable, however, to the average melting enthalpy measured for side-chain methylenes crystallized in the hexagonal form of comblike polyacrylates and polyacrylamides (as well as for the hexagonal-to-liquid transition exhibited by linear alkanes at temperatures close to their melting points), reported to be between 700 and 750 cal CH_2-mol^{-1}.[18] It seems, therefore, that crystallization from the melt in the DL series is not only less hindered than in the D series, but that the hexagonal structure in which the side chains are packed is much better formed. In contrast, a *k* value of about 1200 cal CH_2-mol^{-1} is obtained for the regression straight line obtained from data of the two series together (Figure 3b). Such a value is slightly higher than expected, and it reveals the presence of a well-developed rhombic phase for PAAG-*n* samples obtained by precipitation from solution. In this case, however, the dispersion of data is wider than in the case of melt-crystallized samples, probably due to the uncontrolled annealing that unavoidably affects the samples while handling before DSC running.

The average number of crystallized methylenes calculated using eq 1 for precipitated samples ranges from 1 for PAA(DL)G-14 to 10.0 for PAA(DL)G-22. This range moves down to 0.4−8.6 for melt-crystallized samples. The specific values found for each polymer are given in Table 2, and their variation as a function of *n* values averaged for the two series is plotted against *n* in Figure 4.

A second endotherm with a very weak associated enthalpy was detected in the traces of PAAG-*n* for $n \geq 18$ at a temperature T_2 near 100 °C. The DSC heating scans of annealed samples of PAA(DL)G-18, -20, and -22 showing this endotherm are comparatively shown in Figure 2, together with the evolution that the peak

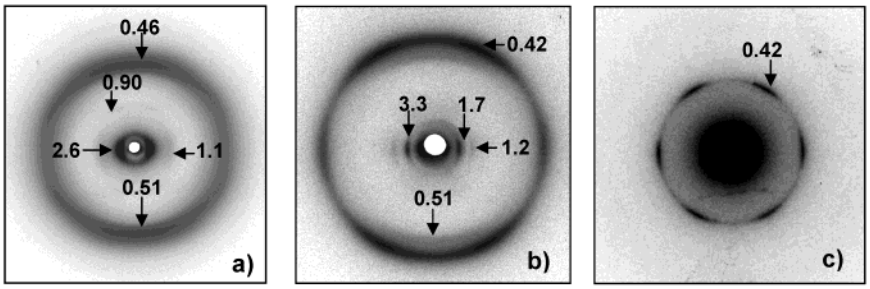

Figure 5. X-ray diffraction patterns of PAA(DL)G-12 (a) and PAA(DL)G-20 (b) stretched oriented films and electron diffraction pattern of a cast film of PAA(DL)G-22 (c).

Table 3. X-ray Diffraction Spacings (nm) of Comblike Poly(γ-glutamate)s at Different Temperatures

	PAAG-12		PAAG-14		PAAG-16		PAAG-18		PAAG-20		PAAG-22	
T (°C)	D	DL	D	DL	D	DL	D	DL	D	DL	D	DL
room (phase A)[a]	3.0	3.0		2.7	2.8	2.8	3.2	3.2	3.5	3.3	3.4	3.7
	2.0	2.0										
	1.50	1.50		1.35	1.40	1.40	1.60	1.60	1.70	1.70	1.70	1.85
	0.45	0.45		0.42	0.42	0.42	0.42[b]	0.42[b]	0.42[b]	0.42[b]	0.42	0.42
80 (phase B)							3.0	3.5	3.0	3.6	3.1	3.9
									1.5	1.9		
							0.45	0.45	0.44	0.46	0.45	0.45
140 (phase C)							2.8	2.7	2.8	2.7	3.0	3.0
							0.46	0.46	0.46	0.46	0.46	0.46
Δd_{A-B} (%)							−6	+9	−15	+9	−14	+8
Δd_{B-C} (%)							−7	−23	0	−25	−3	−23

[a] PAAG-12, -14, and -16 at 20 °C and PAAG-18, -20, and -22 at 37 °C. [b] Weak peak at 0.46 nm observable as a shoulder.

undergoes with the annealing treatment in the case of PAA(DL)G-20. By analogy with both poly(α-glutamate)s[4] and poly(β-aspartate)s,[6] this weak peak could initially be attributed to the occurrence of a second transition leading to a third phase, C. Some distinguishing features of this transition, as it is observed to take place in PAAG-*n*, are the following: (i) T_2 is almost independent of *n*, and its value is about 30 °C lower than that observed for the second transition in PAALA-*n*; (ii) the heat involved in this transition is highly dependent on the enantiomeric content of the polymer, with enthalpy values being up to 10 times larger for the racemic series; and (iii) the transition is dependent on the thermal history—it is a nonreversible process and the associated enthalpy is greatly increased by annealing at temperatures between T_1 and T_2.

The Structure of Phase A. Phase A is the phase present in PAAG-*n* at low temperatures, i.e. below T_1. X-ray diffraction patterns obtained from PAAG-*n* at room temperature were fully consistent with the results obtained by DSC, which were described in the preceding section. Moreover, it was found that these patterns were practically indistinguishable for the D and DL series. For illustrative purposes, the patterns produced by oriented films of PAA(DL)G-12 and PAA(DL)G-22 are shown in Figure 5, and the spacings measured for the whole series are compared in Table 3.

According to current knowledge on the structure of comblike poly(α-glutamate)s[4] and poly(β-aspartate)s,[6] these patterns may be readily interpreted as arising from a two-dimensional supramolecular structure consisting of a layered arrangement of alternating paraffinic and polypeptide phases with the alkyl side chains partially interdigitized. The equatorial reflections with associated spacings between 2.7 and 3.7 nm arise from the layer periodicity of the structure, whereas the strong scattering appearing at 0.40−0.45 nm is produced by the paraffinic phase. For PAA(D)G-*n* with $n \geq 16$ and PAA(DL)G-*n* with $n \geq 14$, this scattering is distributed in a hexagonal array of reflections with a spacing of 0.42 nm, whereas for PAAG-12 and PAA(D)G-14 it is observed as a diffuse ring centered around 0.45 nm. The hexagonal pattern observed in the former case is indicative of a crystallized phase constituted by polymethylene chains packed in a hexagonal array with an interchain distance of 0.48 nm and aligned more or less perpendicular to the layer-planes. Furthermore, the orientation of the 0.42 nm reflections relative to the equator indicates that the hexagonal paraffinic crystal lattice must be oriented with its 100 axis parallel to the stretching direction, i.e., parallel to the main chain axis. These structural features of phase A were confirmed by electron diffraction. The ED pattern shown in Figure 5c was produced by a thin film prepared by casting from chloroform solution of PAA(DL)G-22 on a water surface. Apparently, the alkyl side chains are hexagonally crystallized and are pointing out normal to the film plane, which should be the plane containing the polypeptide layers. On the other hand, the diffuse ring observed in the X-ray diffraction pattern of PAAG-12 and PAA(D)G-14 is consistent with the occurrence of a paraffinic phase in the disordered state, as was anticipated by the DSC analysis. All attempts made to induce ordering in this polymer were unsuccessful. These results allow us to conclude that the hexagonal packing is the arrangement preferentially adopted by the alkyl side chains of PAAG-*n*, that of the rhombic phase being limited to samples crystallized from solution.

As can be seen in the plot shown in Figure 6, the periodicity of the layered structure increases almost linearly with *n*, having a slope near to 0.13 nm per methylene. Since the addition of one methylene in all-trans conformation would entail an enlargement of the layer periodicity by ∼0.24 nm, there is no doubt that interdigitation, and very likely crystallization, of the alkyl side chain increases with *n*. The deviation from

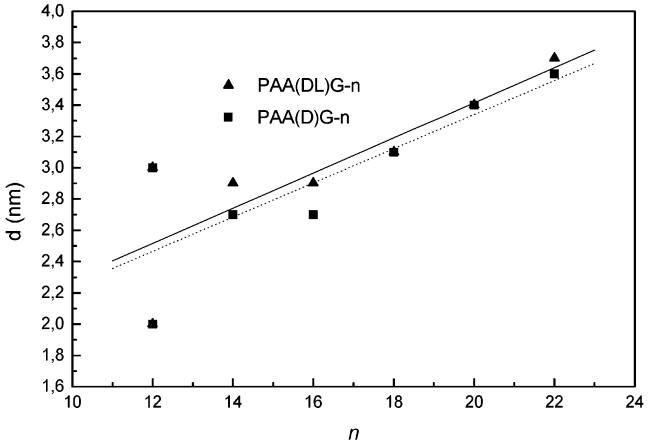

Figure 6. Long spacings of PAAG-*n* against the number of carbon atoms in the alkyl side chain for both D and DL series.

linearity found for PAAG-12 is outside the margin of acceptable experimental error, and could be attributable in principle to the uncrystallized state of the dodecyl side chain. It is noticeable, however, that the spacings of the three reflections observed in the medium-angle region (3.0, 2.0, and 1.5 nm) for this compound, in contrast with those for all the other homologues, are not related by integers, as should be expected for a set of reflections arising from a unique basic spacing. Accordingly, a supramolecular structure with a different type of organization must be adopted in this case. This is not surprising, since poly(α-decyl γ,DL-glutamate)[16] has been found to crystallize in a three-dimensional array characteristic of PGGA-*n* bearing short alkyl side chains.

The conformation adopted by the polypeptide main chain in the layered assembly is an essential feature of the structure that should be determined if a sound description of the whole structure is pursued. This is, however, not an easy matter, since the polypeptide chains are not in crystallographical register, and the X-ray diffraction patterns of the structure appear dominated by the scattering arising from the paraffinic phase. As a result, the X-ray information regarding the polypeptidic phase is obscured and scarce, the only evidence being the meridional scattering appearing at around 0.5 nm. This scattering can be related to the pitch of some of the helical conformations previously described for PAAG-*n*.[9,11]

It is known that poly(γ-glutamate)s bearing benzyl or short alkyl side groups adopt α-helix-type arrangements in both optically pure and racemic varieties.[9,11] Therefore, it is reasonable to assume that the helical conformation is also present in comblike PAAG-*n*, provided that this is the situation encountered in both PA-ALA-*n* and PGAG-*n*. In fact, polarizing infrared spectroscopy has proven without ambiguity that the peptide groups in oriented films of PAAG-*n* are aligned with the C═O and N−H polar vectors parallel to the stretching direction. The normal and parallel dichroic spectra of PAA(D)G-14 and PAA(DL)G-18 are reproduced in Figure 7, showing that the amide A and amide I bands exhibit parallel dichroism, whereas the opposite is observed for the amide II band. This result is taken as solid evidence for the occurrence of a regular folded conformation stabilized by intramolecular hydrogen bonds.

Further evidence supporting the helical structure of the polypeptide main chain in these systems is provided by NMR analysis in the solid state. The ^{13}C CP/MAS

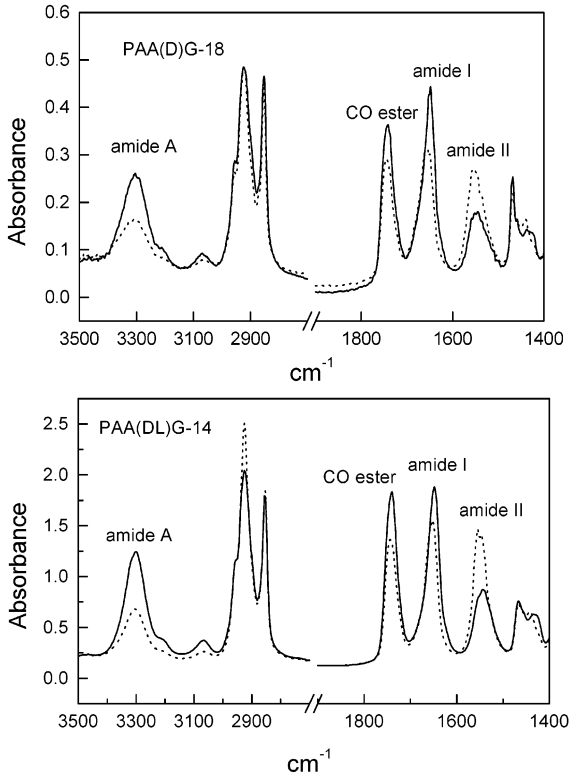

Figure 7. Dichroism infrared spectra of PAA(D)G-18 (top) and PA(DL)G-14 (bottom). Solid line: parallel. Dashed line: perpendicular.

NMR spectra of the PAA(DL)G-*n* series are shown in Figure 8, which includes the spectra of the two crystal forms known for the short alkyl side chain PAA(DL)G-2.[19]

Significant differences are seen between the spectra of comblike PAA(DL)G-*n*, which can be related to the differences in the degree of order assumed by the alkyl side chain depending on its size. What is relevant to the main chain conformation is how these spectra compare with those of PAA(DL)G-2, specifically as far as the carbonyl peak appearing at around 172 ppm is concerned. In the spectrum of PAAG-2, this peak is split in form III (2/1 helices with intermolecular H-bonds) whereas it is not in form II ($^5/_2$ helix with intramolecular H-bonds). Since this signal appears as a single peak for all comblike PAAG-*n*, it can be concluded that these polymers must be in a helical conformation close to form II of PAAG-2. The chemical shifts observed for PGGA-*n* and other related compounds used as references are listed in Table 4.

The A—B Transition. The Structure of Phase B. As revealed by DSC, heating of phase A above T_1 led to phase B. This transition is accompanied by significant changes in the spacings of the structure which can be followed by X-ray diffraction. The powder X-ray diffraction profiles obtained for PAA(D)G-20 and PAA(DL)G-20 at temperatures from 25 to 140 °C are shown in Figure 9. In both cases, the sharp peak at 0.42 nm changes into a broad peak shifted to 0.46 nm upon heating at 80 °C. This change clearly corresponds to the melting of the polymethylene side chain, a process which is found to happen in a similar way for PAAG-*n* with $n \geq 18$.

In the small-angle region, the observed changes clearly differ however for the D and DL series. Thus, in PAA(D)G-20, the 3.5 nm interlayer spacing character-

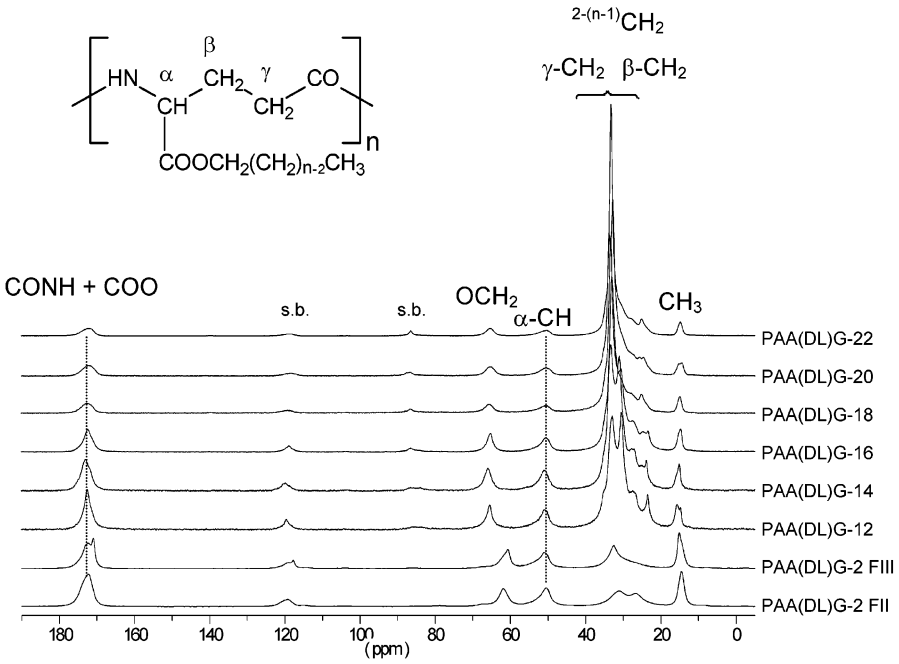

Figure 8. ^{13}C CP/MAS NMR spectra of the PAAG-*n* series recorded at room temperature. Spectra of crystal forms of PAAG-2 are shown for comparison. (s.b., satellite bands).

Table 4. 75.5 MHz ^{13}C CP/MAS NMR Chemical Shifts (ppm) of PAA(DL)G-*n* at Different Temperatures

PAAG-*n*	*T* (°C)	$CO_{amide}+CO_{ester}$	OCH_2	α-CH	$CH_{2(int)}$		$^3CH_2$		CH_2 CH_3	CH_3	
PAAG-12	25	172.5	65.4	50.9	32.9	30.4	27.4		23.4	14.7	15.6
PAAG-14	25	173.0	65.9	50.9	33.2	31.0	27.7		23.8	15.0	
PAAG-16	25	172.4	65.2	50.5	33.0	30.7			23.6	14.8	
PAAG-18	25	172.6	65.5	50.4	33.3			25.0		14.8	
	40	172.6	65.5	50.6	33.3	30.7		25.1		14.9	
	50	173.1	66.0	50.9	33.4	30.8	26.9	25.1	23.6	14.9	
	60	171.9 170.8	65.1	50.6		29.7	26.9	25.8	23.6	14.9	13.8
	70	172.0 170.9	65.2	50.0		29.8		25.9	22.6	13.8	
	80	172.2 171.1	65.4	50.1		29.9	26.0		22.7	13.9	
PAAG-20	25	171.8	65.2	50.2	33.1			25.0		14.7	
PAAG-22	25	172.0	65.3	50.4	33.2			25.0		14.7	
n-alkanes[a]											
$C_{19}H_{40}$ (HEX)					33.7			25.0		14.8	
$C_{20}H_{42}$ (TRIC)				34.9				26.6		16.0	
$C_{23}H_{48}$ (RHOM)				33.6				25.6		15.1	
$C_{23}H_{48}$ (liquid)					29.7				22.6	14.1	

[a] Reference 20. β-CH_2+ γ-CH_2: overlapping with the CH_2(int) peak.

istic of phase A decreased to 3.0 nm in phase B, revealing a compression of the structure in the *a*-direction concomitant with the melting of the paraffinic phase. In contrast, the interlayer distance of PAA(DL)G-20 in phase A, also 3.3 nm, increased to 3.6 nm when the A−B transition took place. The same pattern of behavior is observed for the enantiomorph pairs of PAAG-18 and PAAG-22, with expansions having similar magnitudes for the three members but with contractions being more severe as the value of *n* increases. It should be noticed that a contraction of the layered structure is also observed in the A−B transition of enantiomerically homogeneous PAALA-*n* and PGAG-*n*. Unfortunately, no data are available on the racemic modifications of these systems to see how they compare for the DL series. The diffraction data obtained in this analysis for PAAG-18, -20, and -22 are listed in Table 3.

The description that can be given for phase B is far less complete than for phase A, due essentially to the higher degree of disorder present in this phase and to the inherent technical limitations for the higher domain of temperatures in which this phase exists. The persistence of the well-defined equatorial scattering at temperatures above T_1 reflection is taken as indicative of the occurrence of the layered arrangement. The ^{13}C CP/MAS NMR spectra recorded for PAA(DL)G-18 at increasing temperatures from 20 to 80 °C are shown in Figure 10. A close inspection of these spectra reveals significant differences in the region of alkyl side chain resonances, with an abrupt change taking place around 50 °C, i.e. near T_1. The peak arising from the interior methylenes, with a chemical shift of 33 ppm at low temperature, moved down to 30 ppm at higher temperatures after splitting at 50 °C. The low-field peak is attributed to methylenes in the trans conformation, whereas the high-field peak arises from a mixed population of trans and gauche methylenes characteristic of the molten state. Accordingly, the methyl peak at 15 ppm vanished as a consequence of the enhanced mobility that end groups seem to acquire in phase B. The DIR spectra of PAA(DL)G-14 at room temperature—at which the phase B of this polymer is assumed to be present—is shown in Figure 7, revealing exactly the same dichroic properties as the phase A of PAA(DL)G-20. This result

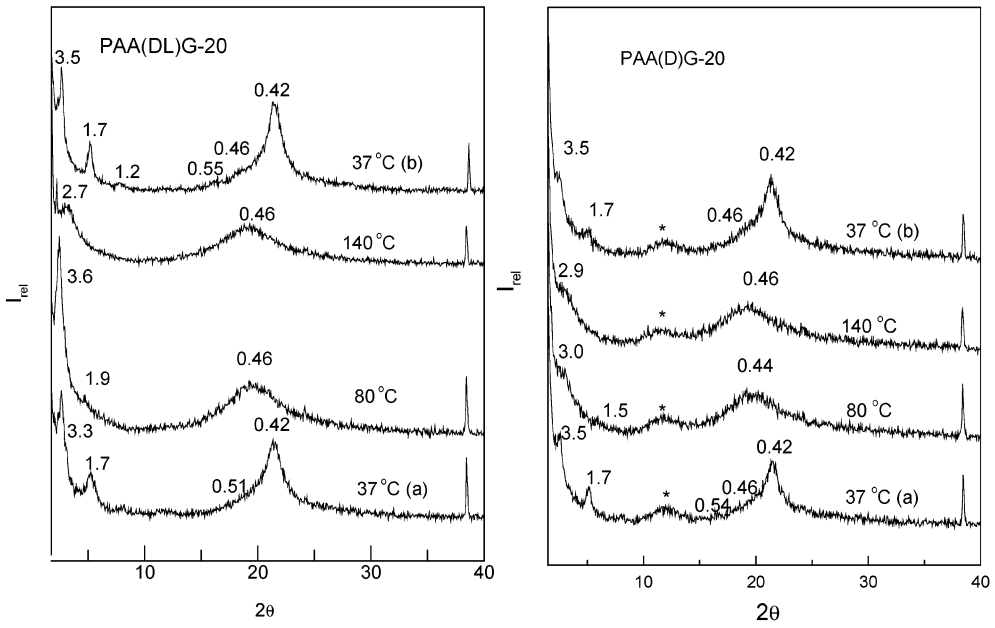

Figure 9. Powder X-ray diffraction profiles of PAAG-20 at the indicated temperatures. (★) Peak arising from silicone glue.

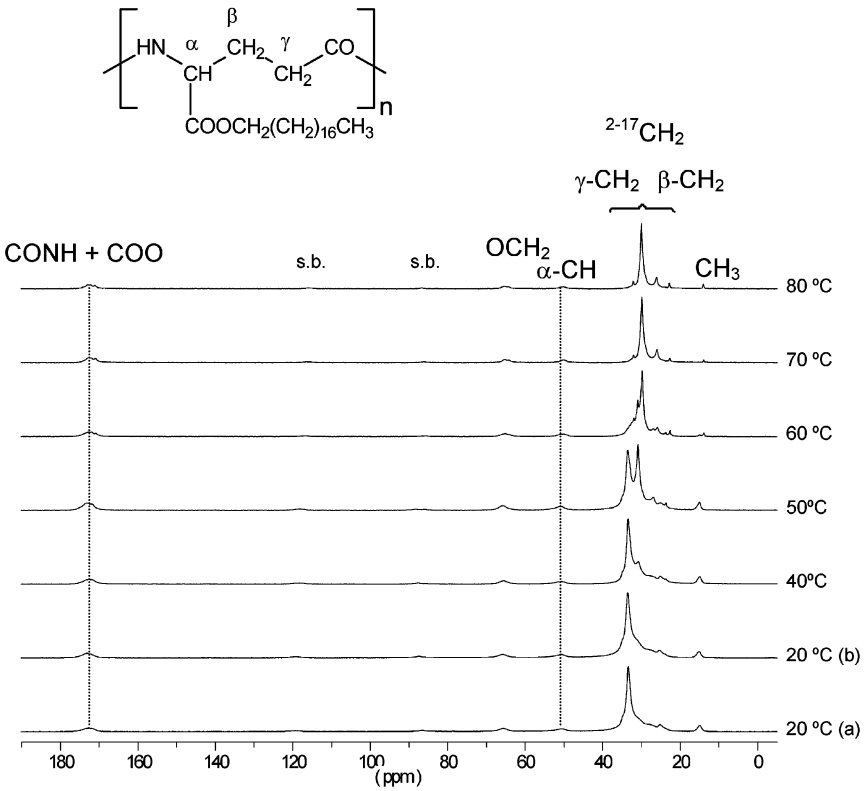

Figure 10. ^{13}C CP/MAS NMR spectra of PAA(DL)G-18 at the indicated temperatures. (s.b., satellite bands).

strongly supports the idea that the conformation of the main chain is the same in both phases A and B. Such a conclusion is further supported by ^{13}C CP/MAS NMR. A close comparison between the spectra of phase A and B did not reveal any difference either in the chemical shifts or in the intensities of the signals arising from the main chain carbons. A computer simulation study on the phase B of PAAG-18, showing that the structure of this phase is consistent with a layered structure of 17/5 or 37/10 helices having alkyl side chains in the molten state but retaining a significant population of torsion angles in trans conformation, has recently been published.[21]

Figure 11 closely compares the spectra recorded for PAA(D)G-20 and PAA(DL)G-20 below and above T_1, i.e. in phase A and B. No difference distinguishing between the D and DL polymers is perceivable for either phase. In fact, none of the data obtained so far show any sign indicating that the structure of phases A and B is different for the PAA(D)G-*n* and the PAA(DL)G-*n* series. This is perfectly acceptable, taking into account the block microstructure that is known to occur in these bacterial poly(γ-glutamic acid) stereocopolyesters.[12] However, the opposite behavior observed in the A−B transition for the two series with regard to density changes would make the finding of some difference between

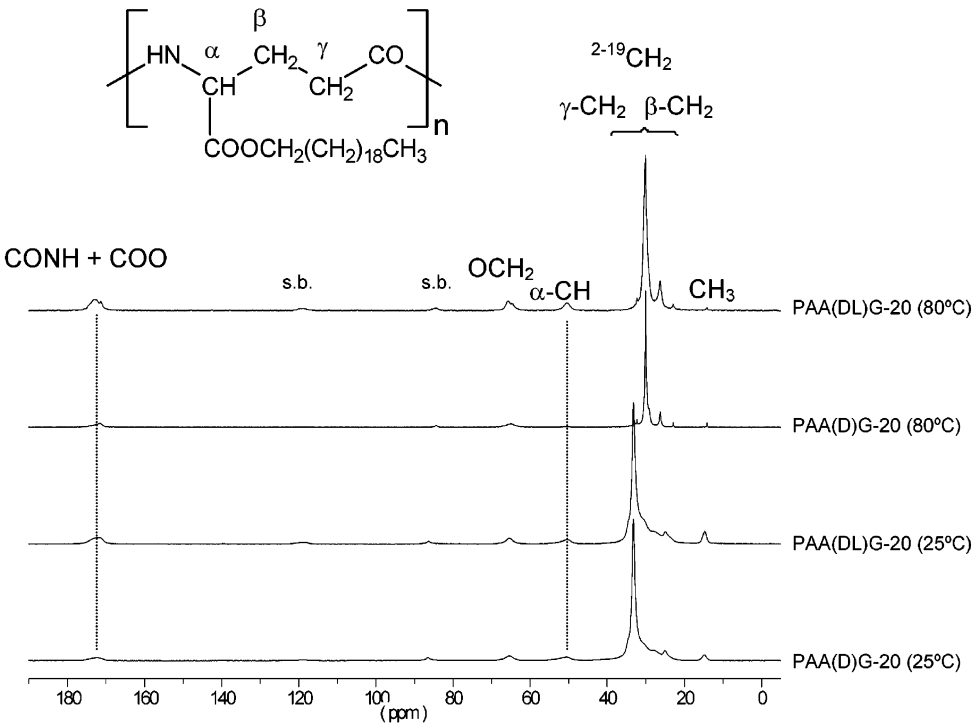

Figure 11. ^{13}C CP/MAS NMR spectra of PAA(DL)G-20 and PAA(D)G-20 at the indicated temperatures. (s.b., satellite bands).

them expected. We conclude that any such difference must be subtle enough to escape the analytical procedures applied in this work. So far, we have no explanation to offer for this striking difference of behavior, which must be correlated to the stereochemical microstructure of the polymer.

The B—C Transition. Close inspection of the DSC heating traces produced by PAAG-18, −20, and −22 reveals the presence of a small endotherm at a temperature T_2 around 100 °C (insets in Figure 2). Annealing at a temperature above T_1 caused the heat exchange associated with this peak to increase, whereas the position of the peak remained essentially unaffected. By trial and error, we found that a maximum enthalpy was obtained upon treatment at 88 °C for 8 days. The T_2 and ΔH_2 values obtained after such treatment are given in Table 2. A second thermal transition takes place therefore at T_2 with generation of a third phase C. The amount of heat associated with this transition is up to one order of times larger for the PAA(DL)G-*n* series than for the PAA(D)G-*n*, to the point that no exchange could be observed for PAA(D)G-18.

The structural changes taking place in this second transition were reflected in the X-ray diffractograms recorded at temperatures between 80 and 140 °C (Figure 9). No appreciable change in the 0.45 nm peak was detected, whereas the interlayer spacing decreased markedly to a value near 2.8−2.9 nm and broadened for all three compounds. It seems, therefore, that the conformation of the main chain is not significantly altered when phase B converts into phase C, whereas the long period of the structure diminishes and simultaneously loses definition. According to what happens in PGAG-*n* and PAALA-*n*, phase C can be envisaged as a nematic phase made up of helical polypeptide rods packed in a quasi-hexagonal array, with an average interchain distance of 2.7 nm. The density calculated for this structure ranges between 0.9 and 1.0 g mL^{-1}, in agreement with what can be expected from experimental data.

Concluding Remarks

Comblike poly(α-alkyl γ-glutamate)s, either enantiomerically enriched or nearly racemic, are shown to adopt a biphasic structure described as a layered arrangement of backbone helical rods embedded in a paraffinic pool made up of polymethylene side chains. One first-order transition—taking place at a temperature T_1 and separating two structurally distinct phases, A and B—was characterized for $n \geq 14$ for the DL series and for $n \geq 14$ for the D series. In phase A, side chains are interdigitized and packed in a hexagonal or a rhombic structure with the fraction of crystallized methylene units ranging between 1 and 9. A better crystallizability was observed for the DL series respect to the D series, which is contrary to what could be reasonably expected. The supramolecular arrangement in phase B was similar to that in phase A, but with the side chains in the molten state. The conversion of phase A into phase B was found to entail a slight contraction of the interlayer distance for the case of the D-series, similarly to what is observed in comblike poly(α-alkyl-β,L-aspartate)s. In contrast, an expansion of the structure takes place throughout the A−B transition in the D-series. The opposite thermal behavior found for PAA(D)G-*n* and PAA(DL)G-*n* is a striking and interesting finding that seems to be related with the enantiomeric composition of the system. A second transition, leading to a third phase C and implying a contraction of the structure, is observed at temperatures T_2 near 100 °C for both PAA(D)G-*n* and PAA(DL)G-*n* with $n \geq 18$. The heat exchange involved in this second transition is much more noticeable for the racemic polymers. By analogy to other comblike polypeptides, phase C is envisaged as a nematic-like structure consisting of a side-by-side packing of polypeptide chains lacking axial register and with side chains in a completely disordered state. The

conformation of the main polypeptide chain is of α-helix type with hydrogen bonds set intramolecularly, and this conformation seems to be retained in the three phases.

Acknowledgment. Thanks are given to Dr. Kubota of Meiji Co. for providing PGGA samples. Financial support to this work was given by DGICYT (Grant no. PB-99-0490).

References and Notes

(1) Loos, K.; Muñoz-Guerra, S. Microstructure and Crystallization of Comb-Like and Block Rigid-Coil Copolymers In *Supramolecular Polymers* 7; Ciferri, A., Ed.; Marcel Dekker: New York, 2000; 269−321.
(2) Watanabe, J.; Goto, M.; Nagase, T. *Macromolecules* **1987**, *20*, 298.
(3) Muñoz-Guerra, S.; López-Carrasquero, F.; Alemán, C.; Morillo, M.; Castelletto, V.; Hamley, I. *Adv. Mater.* **2002**, *14*, 203.
(4) Watanabe, J.; Ono, H.; Uematsu, I.; Abe, A. *Macromolecules* **1985**, *18*, 2141.
(5) Daly, W. H.; Poché, D.; Negulescu, I. *Prog. Polym. Sci.* **1994**, *19*, 79.
(6) López-Carrasquero, F.; Montserrat, S.; Martínez de Ilarduya, A.; Muñoz- Guerra, S. *Macromolecules* **1995**, *28*, 5535.
(7) (a) Fernández-Santín, J. M.; Aymamí, J.; Rodríguez-Galán, A.; Muñoz-Guerra, S.; Subirana, J. A. *Nature (London)* **1984**, *311*, 53. (b) Muñoz-Guerra, S.; López-Carrasquero, F.; Fernández-Santín, J. M.; Subirana, J. A. In *Polymeric Materials Encyclopedia*; Salamone, J. C., Ed.; CRC Press: Boca Raton, FL, 1996; Vol 6, p 4694.
(8) (a) Seebach, D.; Overhand, M.; Kühnle F. N. M.; Martinoni, B. *Helv. Chim. Acta* **1996**, *79*, 913. (b) Appella, D. H.; Cristianson, L. A.; Karle, I. L.; Powell, D. R.; Gellman, S. H. *J. Am. Chem. Soc.* **1996**, *118*, 13071. (c) Hanessian, S.; Luo, X.-H.; Schaum, R.; Michnick, S. *J. Am. Chem. Soc.* **1998**, *120*, 8569.
(9) Puiggalí, J.; Muñoz-Guerra, S.; Rodríguez Galán, A.; Alegre, C.; Subirana, J. A. *Makromol. Chem., Macromol. Symp.* **1988**, *20/21*, 167.
(10) (a) Hintermann, T.; Gademann, K.; Jaun, B.; Seebach, D. *Helv. Chim. Acta* **1998**, *81*, 983. (b) Brenner, M.; Seebach, D. *Helv. Chim. Acta* **2001**, *84*, 2155.
(11) Melis, J.; Zanuy, D.; García-Alvarez, M.; Alemán, C.; Muñoz-Guerra, S. *Macromolecules* **2002**, *35*, 8774.
(12) Martínez de Ilarduya, A.; Ittobane, N.; Bermúdez, M.; Alla, A.; ElIdrissi, M.; Muñoz-Guerra, S. *Biomacromolecules* **2002**, *3*, 1078.
(13) Zanuy, D.; Alemán, C.; Muñoz-Guerra, S. *Int. J. Biol. Macrom.* **1998**, *23*, 175−184.
(14) Morillo, M.; Martínez de Ilarduya, A.; Muñoz-Guerra, S. *Macromolecules* **2001**, *34*, 7868.
(15) Pérez-Camero, G.; Congregado, F.; Bou, J. J.; Muñoz-Guerra, S. *Biotechnol. Bioeng.* **1999**, *63*, 109.
(16) Flory, P. J.; Vrij, A. *J. Am. Chem. Soc.* **1963**, *85*, 3548.
(17) Jordan, E. F.; Feldeisen, D. W.; Wrigley, A. N. *J. Polym. Sci., Part A-1* **1971**, *9*, 1835.
(18) Broadhurst, M. G. *J. Res. Nat. Bur. Stand.* **1962**, *66a*, 241.
(19) Morillo, M. Ph.D. Dissertation, Technological University of Catalonia, 2002.
(20) VanderHart, D. L. *J. Magn. Reson.* **1981**, *44*, 117.
(21) Curco, D.; Zanuy, D.; Alemán C.; Rudé, E.; Muñoz-Guerra, S. *Biomacromolecules* **2003**, *4*, 87.

MA0345201